THE EUROPEAN SOCIETY OF MEDICINE
Medical Research Archives, Volume 12 Issue 9

RESEARCH ARTICLE

# Lymphatic and Blood Vessels in Normal Rhesus Monkey Organs by Immunohistochemical Staining with Frozen Sections: Structure and Function Relationship

**Tatsuo Tomita[1] and Kunie Mah[2]**

[1]Department of Integrative Biosciences, Oregon Health and Science University, Portland, OR, USA and
[2]Oregon National Primate Research Center, Beaverton, OR 97006, USA

OPEN ACCESS

PUBLISHED
30 September 2024

CITATION
Tomita, T. and Mah, K., 2024. Lymphatic and Blood Vessels in Normal Rhesus Monkey Organs by Immunohistochemical Staining with Frozen Sections: Structure and Function Relationship. Medical Research Archives, [online] 12(9). https://doi.org/10.18103/mra.v12i9.5792



DOI
https://doi.org/10.18103/mra.v12i9.5792

ISSN
2375-1924

## ABSTRACT

Practically every organ is supplied by lymphatic and blood vessels, but the presence of these vessels remains elusive at histological level, even using immunohistochemical staining. Currently available immunohistochemical information on lymphatic and blood vessels had derived from data using the routinely formalin-fixed and paraffin-embedded tissue sections. We have performed immunochemical staining for lymphatic and blood vessels using frozen sections aiming to compare our data with previously reported results and to explore new information which has not been reported before. We used LYVE-1 for lymphatic vessels and von Willebrand factor for blood vessels. We studied more than one dozen normal tissues of non-human primate, rhesus monkey, including spleen, lymph node, heart, lungs, intestines, diaphragm, liver, pancreas, thyroid, ovary, prostate, kidney, and urinary bladder. Splenic sinusoids were lymphoreticular and blood vessels in structure and function. Lymphatic sinusoids were immunostained for LYVE-1 only and hepatic sinusoids were positive for LYVE-1 only. In the lungs, lymphatic vessels were diffusely distributed while von Willebrand factor immunostained onto the peripheral alveolar epithelia. In the normal colon, some lymphatic vessels were immunostained in the lamina propria. In the liver, sinusoids were diffusely immunostained for LYVE-1 in the frozen sections. In the kidney, glomerular epithelia were diffusely immunostained for von Willebrand factor. We found lymphatic and blood vessels were superiorly immunostained using frozen sections than using paraffin-embedded sections. Thus, frozen section immunohistochemical staining will superiorly depict lymphatic and blood vessels in normal organ tissues which had not been detected using the formalin-fixed and paraffin-embedded sections before. More immunohistochemical information will forthcomimg using frozen sections. From our results, we conclude the significance of lymphatic and blood vascular system is unique for each organ in structure and function.

**Keywords:** Blood vessels, immunohistochemistry, frozen sections, lymphatic vessels, LYVE-1, rhesus monkey, von Willebrand factor

## Introduction

Every organ is supplied by lymphatic vessels except brain, spinal cord, cartilage, bone marrow, eye lens and others[1-3], but the precise presence of lymphatic vessels in each organ is still elusive at histological levels. Using immunohistochemical staining for lymphatic and blood vessels using frozen sections, we immunostained lymphatic and blood vessels with currently available immunohistochemical markers[1-6]. In this study, we have aimed to compare our immunohistochemical data using frozen sections with those previously reported results using the formalin fixed and paraffin-embedded tissue and further to explore new information of lymphatic and blood vascular system which has not been reported before. The currently commercially available markers for lymphatic vessels include proxy-1 (prospero-related hemeobox-1), LYVE-1 (lymphatic vessel endothelial hyaluronic acid factor receptor-1), prodoplanin (43 kDa membrane glycoprotein of podocyte) and VEGER-3 (vascular endothelial growth factor receptor-3). LYVE-1 is a transmembrane receptor for hyaluronin, a highly expressed by lymphatic vessels[3,5,6] and a prodoplanin is a membrane glycoprotein found on the surface of rat glomerular epithelial cells, podocytes, recognized by the monoclonal antibody, D2-40[3]. These markers bind to their own specific binding site indifferent modes and they all function in diverse ways at different stages of tissue growth and development [2,3]. The markers for blood vessels are CD31 (platelet endothelial adhesion molecule PECAM-1, found on endothelial cells), CD34 (single-class transmembrane sialomucin protein, its antibody is used for hematopoietic progenitor cells, positive for blood vessel endothelium but not usually lymphatic vessel endothelium) and von Willebrand factor (vWF, binds factor -8, a clotting factor in blood vessel, platelet aggregation and adhesion to the cell wall of injured vessels), which are all pan-endothelial markers[4]. But there are no specific markers for lymphatic and blood vessels[2,3,7-10]. We had previously performed such immunohistochemical staining with normal organs from rhesus monkey and found that frozen sections were superior for immunostaining lymphatic and blood vessels to the routinely formalin-fixed and paraffin-embedded sections[11]. To anatomic pathologists, it is crucially important to identify precise location of lymphatic and blood vessels in cancerous tissues. The classical staining for blood vessels is van Gieson stain for the lining elastica for distinguishing blood vessels from small tissue space due to fixation artifact in buffered formalin-fixation and paraffin-embedding. The presence of red blood cells in the vessel space supports identifying blood vessels. These two vessels not only supply lymph and blood but have crucial roles in spreading tumor and metastasis. We employed mostly LYVE-1 for lymphatic vessel markers and vWF for blood vessel markers in normal non-human primate, rhesus monkey tissues[9-11].

## Materials and Methods

For frozen sections, normal organ tissues from Macaca mulatta (rhesus monkey) were procured by necropsy at the research laboratory of Drs. Ov Slayden and Robert Brenner at the Oregon Primate National Research Center, Beaverton, OR. The frozen organ tissues included spleen, lymph node, intestines, diaphragm, liver, thyroid, ovary, prostate, kidney, and urinary bladder. Additionally, monkey spleen, liver and kidney were fixed in a mixture of 1% paraformaldehyde and 1% formalin and were embedded in paraffin to compare with frozen section immunostaining. With spleen and liver fixed in the above mixture and embedded in paraffin, double immunohistochemical staining was performed for LYVE-1 and vWF using two colors of brown by diaminobenzidine tetrahydrochloride and blue color by Vectastin and Vector SG (Burlingame, CA). Small fresh tissues (1 x 1 x 0.4 cm) were embedded in OCT matrix (Fisher Scientific, Pittsburgh, PA) and were frozen in liquid propane in the liquid nitrogen bath as described before[12-14] and were frozen sectioned at 5- 7 microns. Frozen sections were mounted on Super Plus slides (Fisher Scientific), microwave-irradiated on ice for 3 sec, fixed in 2% paraformaldehyde in phosphate buffer at pH 7.4

for 10 to 15 min at room temperature and immersed twice for 2 min in 85% ethanol[11-14]. To inhibit endogenous peroxidase activity, sections were incubated with a solution containing glucose oxidase (1U/ml) and sodium azide (10 mmol/ml) in PBS for 45 min at 25°C (11-14). Sections were incubated with blocking serum for 20 min. Then, sections were incubated with each diluted primary antibody solution overnight at 4°C. After rinsing and immersion in blocking serum again, sections were incubated with second antibody (1: 200 dilution) for 30 min at room temperature. Final visualization was achieved with the ABC kit (Vector Laboratory, Burlingame, CA) and 0.025 diaminobenzidine tetrahydrochloride in Tri-buffer pH 7.6, 0.03% $H_2O_2$ to induce brown color. The source of the primary antibodies and each dilution of the antibody for frozen sections and paraffin-embedded tissues were as follows:

| | | Frozen sections | Paraffin-sections |
|---|---|---|---|
| Goat anti-human LYVE-1 | R and D System, Minneapolis, MN | 1: 1,200 | 1: 100 |
| Mouse monoclonal D2-40 | Signet Laboratories, Dedham, Mass | 1: 100 | 1: 100 |
| Rabbit human vWF | Dako System, Carpenteria, CA | 1: 800 | 1: 100 |

## Results

SPLEEN AND LYMPH NODE (Figure 1)

Frozen sections of spleen showed diffuse LYVE-1 immunostaining in the sinusoidal epithelia in the mostly large caliber capillaries with no immunostaining for central arteries in the germinal center while vWF immunostaining revealed positive immunostaining in the small caliber capillaries and central arteries (Fig. 1 -A and -B). The small caliber capillaries were positively vWF immuno-stained with only the frozen sections (Fig. 1-B) but not immunostained with the paraffin-embedded sections (Fig. 1-D). Double immunostaining for LYVE-1 in brown and vWF in blue color was performed with the paraffin-embedded sections, which showed positive LYVE-1 staining in the large caliber capillaries while F-8 positively immunostained central arteries but not in the small caliber capillaries (Fig. 1-D). Thus, there were two sets of capillaries in the red pulp: larger caliber capillaries being positive for LYVE-1 and small caliber capillaries being positive for vWF in the frozen sections (Fig. 1-A and -B). The frozen sections of lymph node showed a few lymphatic vessels in the cortex and there were numerous slender and round lymphatic vessels in the medulla and connective tissues of the hilum (Fig. 1-E). The lymphatic sinusoidal epithelia in the subcapsular (marginal)-medullar junction were positive for LYVE-1 and negative for vWF (Fig. 1-E and -F). With vWF immunostaining, mostly round thick-walled arteries were immunostained while thin-walled veins were stronger immunostained in the medulla and hilum (Fig. 1-F).

HEART AND LUNG (Figure 2)

Heart revealed numerous, diffusely dispersed small lymphatic vessels in full thickness of ventricle excluding endocardium (Fig. 2-A) while cross round sections of scattered small blood vessels were depicted in the entire ventricle by vWF immunostaining in ventricle (Fig. 2-B). Lung showed diffusely distributed small lymphatic vessels supplying into the terminal bronchi (Fig. 2-C) while vWF immunostained diffusely onto the peripheral alveolar surface (Fig. 2-D and –F).

**Figure 1.** Spleen and Lymph Node

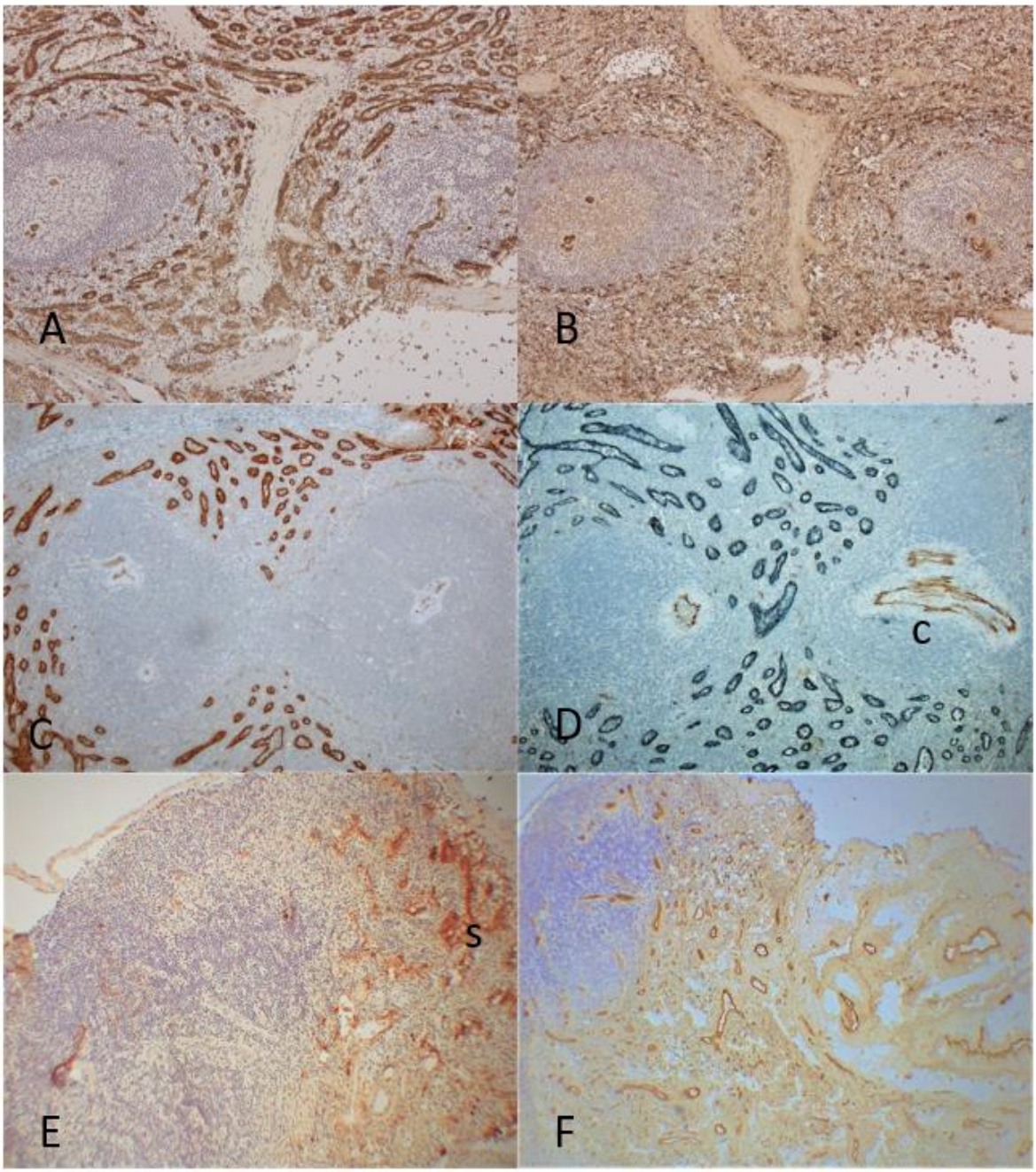


The frozen sections of spleen showed diffuse positive immunostaining in the sinusoids for LYVE-1 in larger caliber capillaries and positive staining for vWF in smaller caliber capillaries (A and B) while central arteries and larger blood vessels were strongly immunostained for vWF (B). The paraffin sections showed strong staining for LYVE-1 in larger capillaries (C) and double staining showed positive staining in larger capillaries for LYVE-1 but negative for vWF while central arteries were positive F-8 but not in sinusoidal capillaries (D).The frozen sections of lymph node showed densely packed LYVE-1 positive lymphatic vessels in the sinusoids and vWF positive blood vessels in medulla and hilar connective tissue (E and F).

A, B, E and F: Frozen sections, C and D: Paraffin-embedded sections

A, C and E: LYVE-1, B and F: vWF, D: LYVE-1 and vWF double immunostained

c: central artery, s: lymphatic sinusoid

**Figure 2.** Heart and Lung

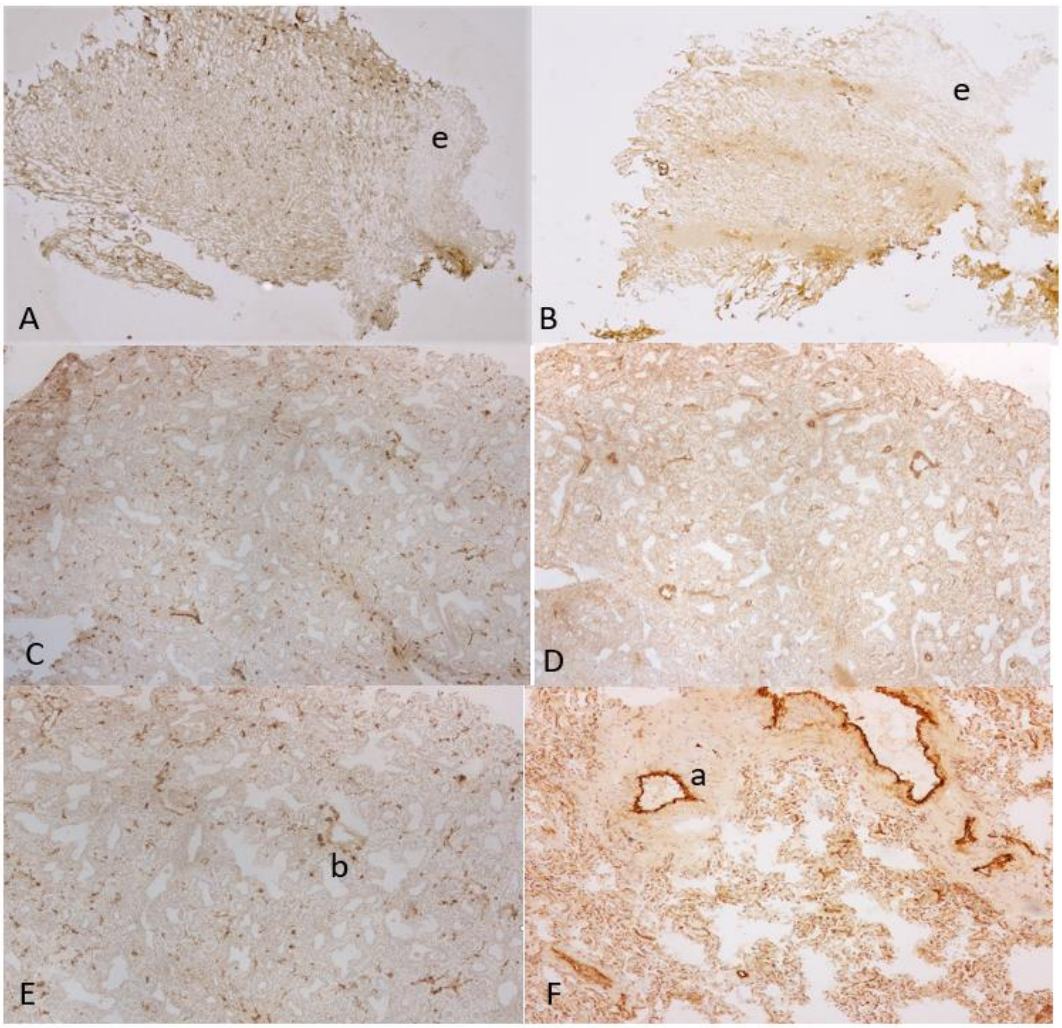


In the sections of ventricle of the heart, there were many scattered small lymphatic vessels in the entire ventricle excluding endocardium while a few blood vessels were immunostained by vWF (A and B). In the lungs, small lymphatic vessels were dispersed into the small bronchial wall (C) while capillaries were diffusely immunostained into the alveolar endothelial surface (E and F).

A, C and E: LYVE-1, B, D and F: vWF immunostained

a: artery, e: endocardium, p: sub-peritoneum, v: vein

SALIVARY GLAND, ESOPHAGUS AND DIAPHRAGM (Figure 3)

In the salivary gland, small linear lymphatic vessels were dispersed in the inter-acinar fine stroma, the lymphoid follicle and around arterioles while larger linear lymphatic vessels surrounded the ducts (Fig. 3-A). Small linear blood vessels were dispersed in the inter-acinar fine stroma, some of which surrounded the ducts while round, plump blood vessels were scattered in the submucosa (Fig. 3-B). In the esophagus, rich small and large linear lymphatic vessels were present in the lamina propria including around the arterial walls (Fig. 3-C). There were many linear and round blood vessels in the lamina propria including the lymphoid follicle in the submucosa (Fig. 3-D). Capillaries were dispersed in the squamous mucosa (Fig. 3-D). There were many small lymphatic vessels and larger blood vessels in the submucosa (fig. 3-C and -D). In the diaphragm, many small lymphatic vessels were depicted in the subserosa by LYVE-1 immunostaining (Fig. 3-E). D2-40 revealed similar immunostaining for lymphatic vessels with moderate staining in the fibrous stroma (Fig. 3-G). There were small lymphatic vessels in the fibrous connective tissue and around the arteries (Fig. 3-E). By vWF immunostaining, both relatively large arteries and veins were depicted in the connective tissue and there were diffusely distributed small capillaries at the margin of the striated muscle bundle (Fig. 3-F).

**Figure 3.** Salivary Gland, Esophagus and Diaphragm

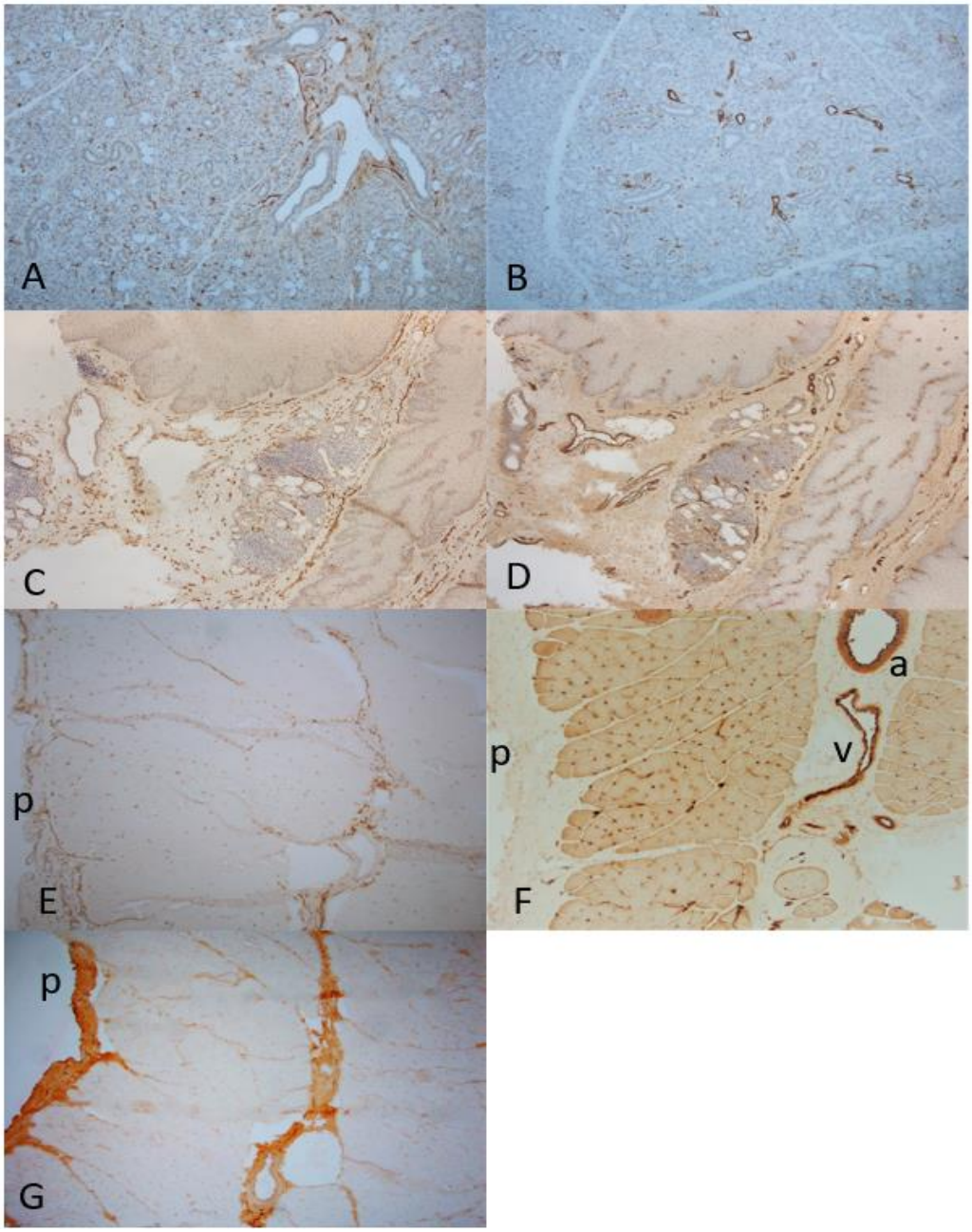


In the salivary gland, small linear lymphatic vessels and round blood vessels were dispersed in the inter-acinar stroma (A and B). In the esophagus, linear small and larger lymphatic vessels and many linear and round blood vessels were in the lamina propria (C and D) including the outer layer of squamous epithelia and lymphatic follicle (C and D). In the diaphragm, there were many small lymphatic vessels in the sub-peritoneum and there were small lymphatic vessels around the small arteries in the fibrous stroma (E). There were also many small blood vessels in the sub-peritoneum and there were numerous capillaries at the margin of muscle bundle (F). Interstitial fibrous stroma was moderately immunostained for D2-40 (G).

A, C and E: LYVE-1, B, D and F: vWF, G: D2-40 immunostained.

A: artery, v: vein, P: peritoneum

DOUDENUM, SMALL AND LARGE INTESTINES (Figure 4)

In the duodenum, linear lymphatic vessels extended into the small villi and aggregates of small lymphatic vessels were dispersed between inner and outer smooth muscle bundles (Fig. 4-A). Small capillaries extended into the tip of the villi and there were numerous dilated blood vessels in submucosa (Fig. 4-B). In jejunum, large dilated lymphatic vessels were depicted in the tall villi (Fig. 4-C) and there were many small capillaries in the villi and were many large round blood vessels in the submucosa (Fig. 4-D). In the

large intestines, there were some linear and vertical lymphatic vessels in lamina propria and abundant larger lymphatic vessels in the submucosa (Fig. 4-E) and lymphatic and blood vessels vertically spread through the smooth muscle layers (Fig. 4-E). There were scattered small capillaries in the lamina propria and numerous larger dilated veins in the submucosa (Fig. 4-G and -H). In the well-fixed normal large intestine with formalin and embedded in paraffin, there were a few linear, vertical lymphatic vessels in the lamina propria and abundant lymphatic vessels in the submucosa (Fig. 4-F).

**Figure 4.** Small and Large Intestines

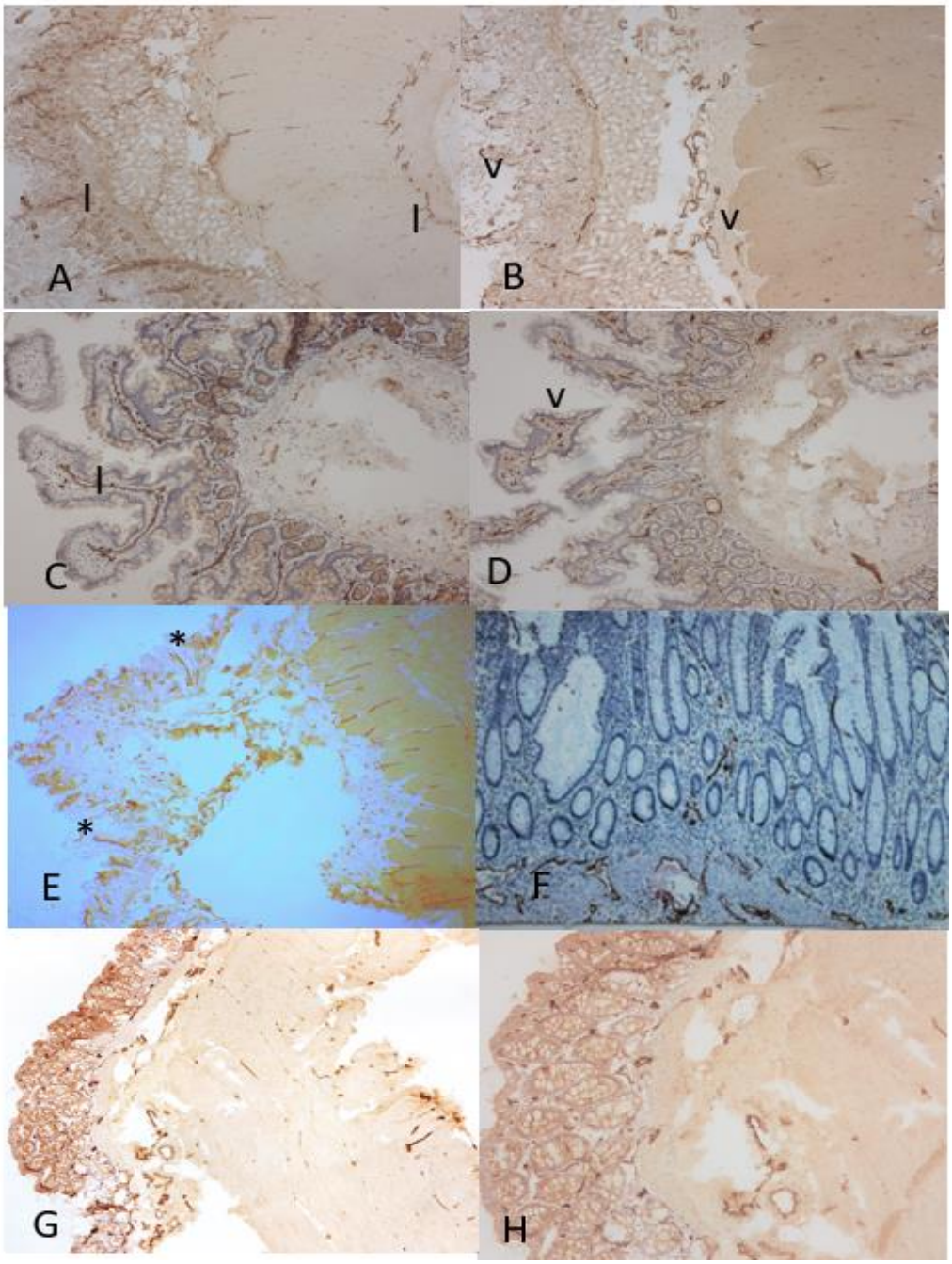


The frozen sections of duodenum showed linear and vertical lymphatic vessels in lamina propria and aggregates of small lymphatic vessels between inner and outer smooth muscle bundles (A). There were scattered small blood vessels in lamina propria and numerous round blood vessels in submucosa (B). The frozen sections of jejunum showed large, tall villi containing dilated lymphatic vessels (C) and small blood vessels (D). There were small lymphatic vessels and round, larger blood vessels in submucosa (C and D). The frozen sections of large intestine showed some vertically extending lymphatic vessels and scattered small blood capillaries in lamina propria (E). There were numerous linear lymphatic vessels and larger, round arteries and veins in submucosa (G and H). The well formalin-fixed and paraffin-embedded sections of large intestine also revealed some linear vertical lymphatic vessels in the lamina propria and abundant linear lymphatic vessels in the submucosa (F).

There were abundant blood vessels in the lamina propria of large intestine (H).
A, C, E and F: LYVE-1, B, D, G and H: vWF immunostained
a: artery, l: lymphatic vessel, v: vein

LIVER AND PANCREAS (Figure 5)

For LYVE-1 immunostaining in the liver, staining between frozen sections and paraffin-embedded sections was compared, showing darker staining in the relatively broader hepatic lobules in frozen sections (Fig. 5-A) compared to the weaker staining in the relatively thinner lobules in the paraffin-embedded liver sections (Fig. 5-B). In frozen sections, sinusoids were diffusely stained for LYVE-1 with stronger stained in pericentral lobe than periportal lobe while pericentral sinusoids were weaker or not stained for LYVE-1 in paraffin-embedded sections (Fig. 5-A and -B). With vWF immunostaining, blood vessels were strongly stained in larger vessels while sinusoids were negative in both frozen sections and paraffin-embedded sections (Fig. 5-C and -D). Double immunostaining for LYVE-1 and vWF showed sinusoidal endothelial staining in brown for LYVE-1 and vWF staining in arteries and veins in blue (Fig. 5-D). In the pancreas, frozen sections showed LYVE-1 barely weakly stained in pancreatic islets with no lymphatic vessels within islets (Fig. 5-E). vWF staining revealed pancreatic islets containing round baskets of abundant, tangled capillaries around and in islets while thick-walled arteries and thin-walled veins were moderately and strongly stained (Fig. 5-F).

**Figure 5.** Liver and Pancreas

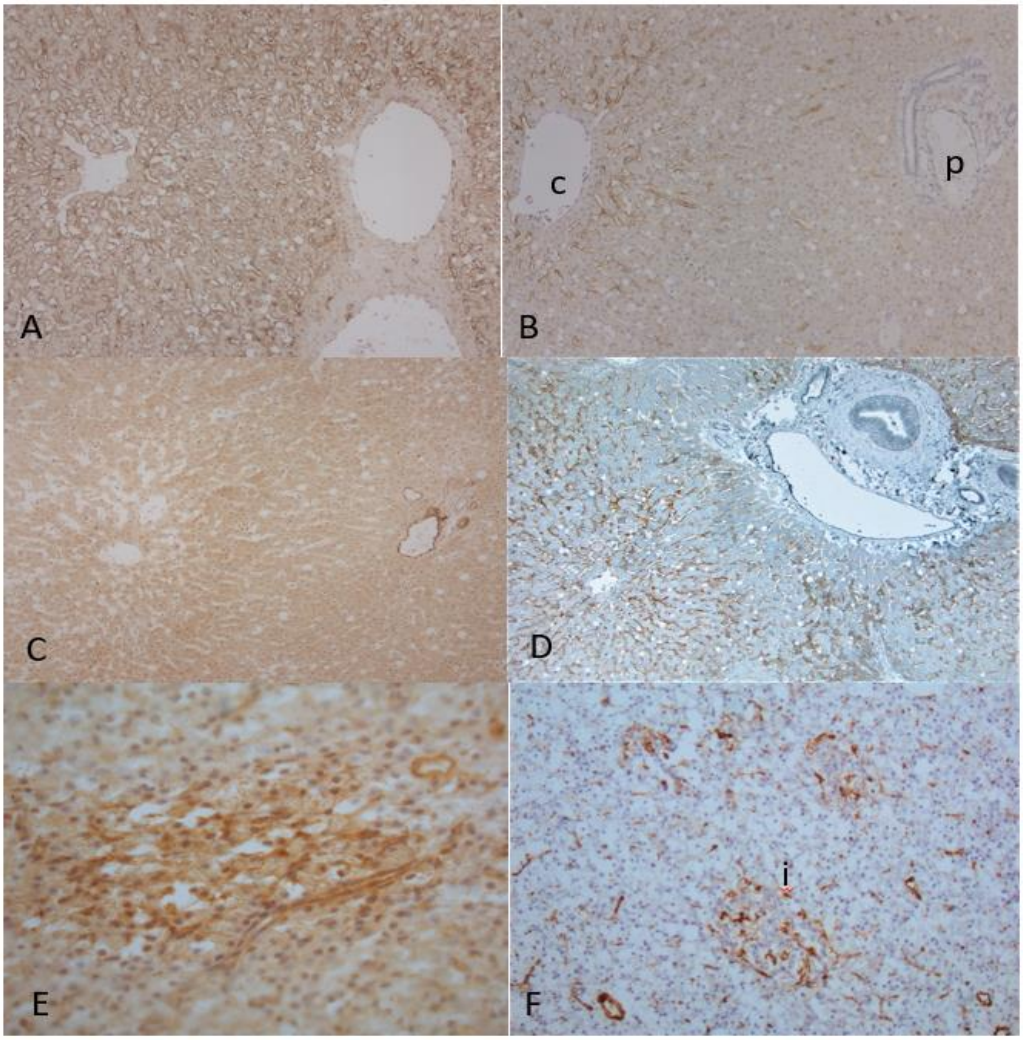


The frozen sections of liver showed stronger LYVE-1 immunostained sinusoids in frozen sections than paraffin-embedded sections (A and B). The LYVE-1 immunostaining was stronger in the pericentral lobe than in periportal lobe, in the latter there was less immunostaining in frozen section and no staining in paraffin-embedded sections (A and B). Frozen sections of liver

immunostained blood vessels only in sinusoids (C). Double immunostaining with paraffin-embedded sections for LYVE-1 and vWF showed LYVE-1 positive staining in sinusoids in brown and F-8 positive staining in arteries and veins in blue (C and D). Frozen sections of pancreas showed diffuse weak staining for LYVE-1 in islets and baskets of numerous, tangled capillaries around and in the islets for vWF immunostaining (E and F).
c: central vein, i: islet, p: portal area
A, C and E: LYVE-1, B and F: F-8, D: LYVE-1 and vWF double immunostained
c: central vein, i: islet, p: portal area

THYROID, OVARY AND PROSTATE (Figure 6)

In the thyroid, there were diffusely scattered, small linear lymphatic vessels in the fine interfollicular connective septa (Fig.6-A) and abundant large thick-walled arteries and thin-walled veins were strongly immunostained for vWF in the broader, fibrous septa (Fig. 6-B). In the ovary, there were diffusely, abundant linear lymphatic vessels and diffusely, abundant more plump venous vessels around Graafian follicles (Fig. 6-C and -D). In the prostate, there were abundant lymphatic and blood vessels in the subcapsular connective tissues where there were abundant nerve bundles (Fig. 6-C and -D). There were some small linear lymphatic vessels, and abundant linear blood vessels in the stroma (Fig. 6-E and-F).

**Figure 6.** Thyroid, Ovary and Prostate

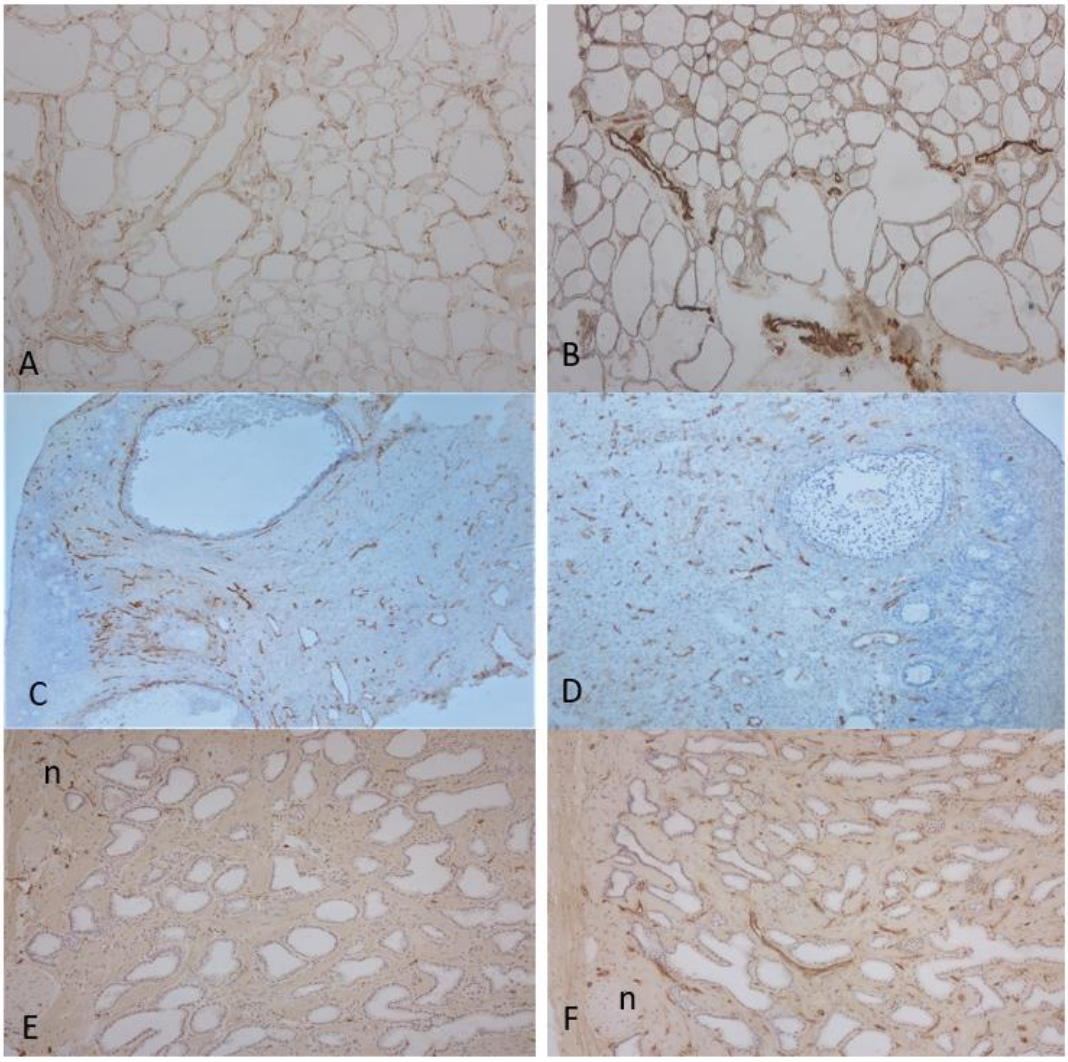


Frozen sections of thyroid showed abundant scattered linear lymphatic vessels in fine fibrous septa (A) and many larger, round blood vessels in the broader septa (B). Ovary showed diffusely, scattered small, linear lymphatic vessels (C) and diffusely, rounder blood vessels around the Graafian follicles in the fibrous stroma (D). Prostate showed many, small linear scattered lymphatic vessels in the sub-capsular and some lymphatic vessels in interstitial stroma (G) and there were numerous small, linear blood vessels in the stroma (F).

A, C and: E LYVE-1, B, D and F: vWF immunostained
a: artery, g: glomerulus, n: neuron, v: vein

ADRENAL, KIDNEY AND URINARY BLADDER (Figure 7)
Adrenal gland contained numerous small lymphatic vessels and larger, dilated blood vessels in the subcapsular tissue (Fig. 7-A and -B). There were a few small lymphatic and blood vessels depicted in the cortical and medullary connective tissue (Fig. 7-A and -B). In the kidney, there were a few linear lymphatic vessels around arterial adventitia (Fig. 7-C and -D) while there were many small linear lymphatic vessels around the blood vessels in the medulla (Fig. 7-E). Glomerular capillaries were diffusely and densely immunostained in full endothelial thickness with vWF, suggestive of the leaking glomerular capillaries immunostained by vWF (Fig. 7-D). D2-40 immunostaining was positive for the Bowman's capsule (Fig. 7-F). In the urinary bladder, there were cross sections of the dispersed small lymphatic and blood vessels in the muscularis mucosa while smooth muscle layers revealed some dispersed lymphatic and blood vessels by vWF immunohistochemical staining (Fig. 7-G and -H).

**Figure 7.** Adrenal, Kidney and Urinary Bladder

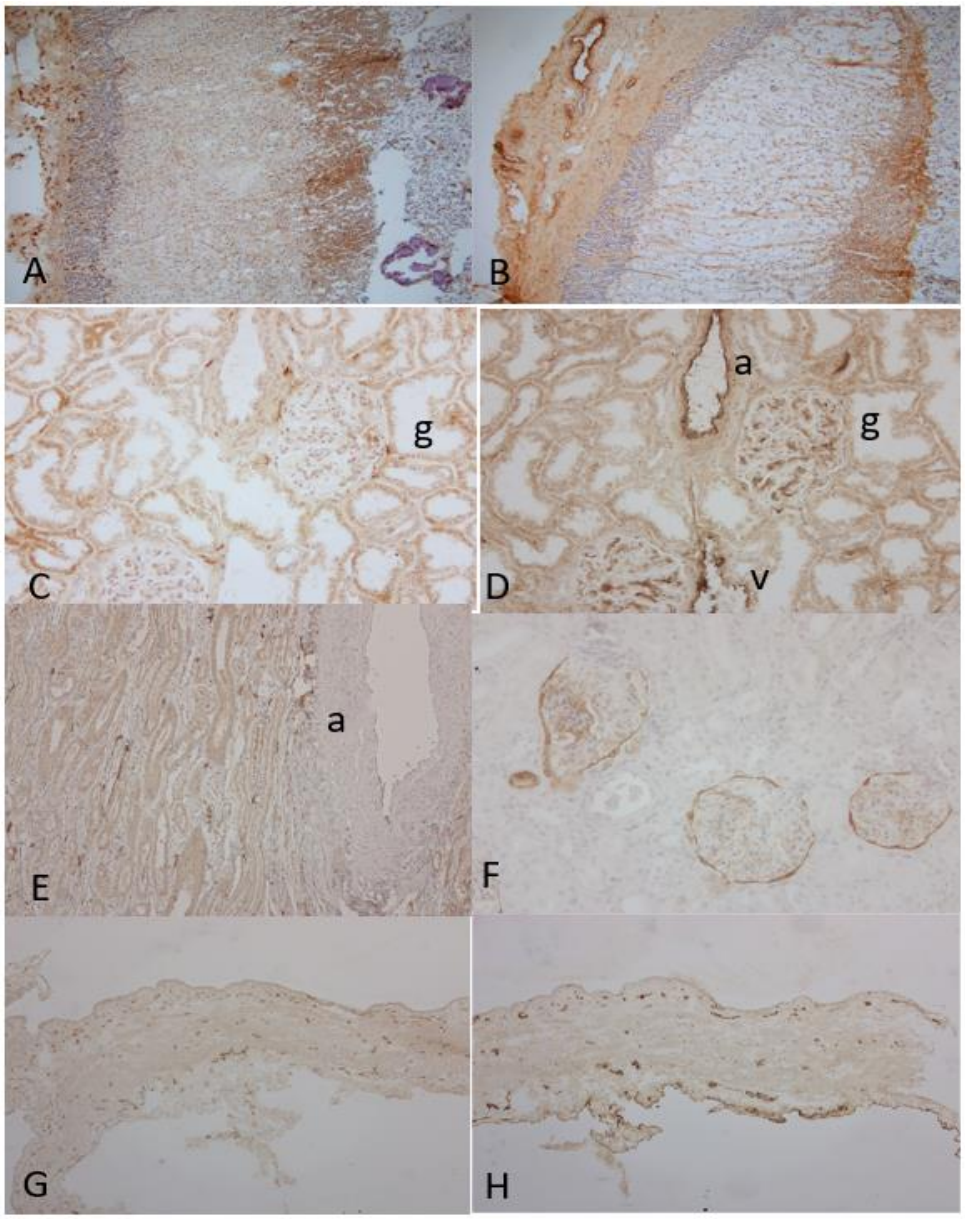


In the adrenal subcapsular stroma, there were many small lymphatic vessels and several arteries and veins while there were no lymphatic and blood vessels in the cortex by both LYVE-1 and F-8 immunostaining (A and B). In the kidney, there were a few small linear lymphatic vessels in the arterial adventitia (C). Glomerular endothelia were diffusely immunostained

in full thickness by vWF, suggestive of leaking serum vWF also immunostained the epithelium of artery and vein (C and D). In the medulla, there were many linear lymphatic vessels around the artery (E). The Bowman's capsule was immunostained by D2-40 (F). In the bladder, there were scattered small lymphatic and blood vessels in the muscaris mucosa, and these were scattered lymphatic and blood vessels in the smooth muscle layers (G and H).
A, C, E and G: LYVE-1, B, D and H: vWF, F: D2-40 immunostained.
a: artery, v: vein

## Discussion

The structure and function relationship of lymphatic vessels has been overshadowed and delayed than that of blood vessels due to a lack of specific markers for lymphatic vessels to date[1,3,5,6]. As shown in the dilution of primary antibodies, frozen sections required a fraction of primary antibodies than using routinely formalin-fixed and paraffin-embedded sections, requiring much more diluted antibodies, especially LYVE-1 and vWF, so immunohistochemical staining with frozen section was much more economical than paraffin-embedded sections since many antibodies are expensive.

The different immunostaining pattern was revealed in the spleen where large caliber capillaries were positive for LYVE-1 and small caliber capillaries were positive for vWF, in the latter small caliber sinusoidal epithelia were positively immunostained in frozen sections but not in paraffin-embedded sections (Fig. 1-B and -D). So, there were two kinds of sinusoidal capillaries in the spleen: large caliber capillaries were LYVE-1 positive lymphatic vessels and small caliber capillaries were vWF positive blood vessels (Fig. 1-A and -B). In studies using paraffin-embedded sections, splenic sinus was reportedly patchy positive for vWF and negative for CD34[4,15-17]. The splenic red pulp is lined by a distinctive endothelial cell with a partial histologic function called splenic litloral cells, which express endothelial markers like F-8, CD31, wT1 (Wilms tumor protein 1), ERG (a member of the erythroblast transformation-specific family) and CD68 (a protein highly expressed by the cells in the monocyte lineage by circulating and tissue macrophages)[15-17]. Blood is sequestrated in the splenic sinus in the red pulp under portal hypertension. The sinusoids of larger caliber capillaries allow transporting whole blood cells between capillary wall and adjacent tissue, and its endothelia increase the attachment of vWF on the splenic litloral cell surface, resulting in strong vWF staining on the surface. Among the two different splenic sinusoidal endothelia, the larger sinuses were lymphatic vessels and smaller caliber endothelia were blood vessels by this immunostaining, so these two capillaries function as both lymphatic and blood vessels, respectively. The sinusoid of human spleen is an unusual vascular structure which is involved in the removal of damaged erythrocytes and permits the migration of leukocytes from the cords into the circulation[15-17]. This sinusoidal epithelium is equivalent to the other endothelium in their immunoreactivity to vWF and HLADR antigens[15-17]. The white splenic pulp, germinal center contains central arteries (Fig. 1-D) which is surrounded by lymphoid cells, the so-called periarterial sheath (PALS) and adjacent outpouching of nodular lymphoid tissue[3,4,15-17]. The lymph node sections showed a specific pattern for lymphoid sinusoids, which were positive only for LYVE-1 (Fig. 1-E). The lymphoid sinus is located at the subcortical (marginal) -medullary junction (Fig. 1-E). Lymph nodes filter protein-rich lymph fluid through lymphatic sinusoids while spleen filters blood through splenic sinusoids[3,4]. In lymph node, there are abundant arteries and veins in medullary cord and hilus with small lymphatic vessels in the periarterial stroma (Fig. 1-E and –F).

The sections of the cardiac ventricle showed numerous small dispersed lymphatic vessels in full thickness while there were less blood vessels depicted (Fig. 2-A and-B). Cardiac lymphatics consist of terminal capillaries and these capillary form plexuses that drain continuously subendocardial, myocardial, and subepicardial areas, and draining lymphatic vessels lead the lymph out of the heart[18]. The diffusely distributed small lymphatic vessels correspond to the terminal lymphatic capillaries. The heart is richly

supplied with capillaries, run in parallel between cardiac muscle bundles consisting of several cardiac myocytes[19]. Sections of lung showed diffusely distributed lymphatic vessels into the alveolar sac while alveolar epithelial surface was immunostained by vWF (Fig. 2-C and -D). Using Prox-1, podoplanin and LYVE-1, lymphatic vessels were depicted inside the pulmonary lobules associated with bronchioles, interlobular arterioles, and small veins and interlobular lymphatic vessels were in close contact with blood vessels[20]. Numerous small perivascular lymphatic vessels probably absorb compartment of the lung responsible for maintaining alveolar interstitium relatively dry to provide the minimal thickness of air-blood barrier to optimize gas diffusion[20]. These rich lymphatic vessels also contribute easy lymphatic spread of primary pulmonary carcinoma and metastatic carcinoma[20].

Aiyama et al studied rat salivary gland with frozen section immunostaining using monoclonal antibody against rat podoplanin[21]. Lymphatic vessels were found in the interlobular stroma and around interlobular ducts[21]. Linear and round blood vessels were richly distributed in the salivary gland including ductal walls. In the esophagus, Yajin et al reported dense lymphatic vessels in lamina propria with most of them longitudinally[22]. We depicted richly distributed linear lymphatic vessels in the esophageal lamina propria. There were also many round blood vessels in the lamina propria including around arterial wall and lymphoid follicle.

Sections of diaphragm showed aggregates of small lymphatic vessels in sub-peritoneum and fine fibrous stroma while there were numerous small capillaries in the margin of striated muscle and there were abundant blood vessel networks in the broad fibrous septa (Fig. 2-E and -F). This rich blood vessel network is thought to be responsible for hematogenous spread of lung cancer to adrenal gland, which accounts for 40% of adrenal metastasis[23-25]. The route of lung cancer metastasis to adrenal glands is still debated, mainly lymphatic route in the early stage of cancer and hematogenous spread in the late stage of cancer[24,25].

The frozen sections of duodenum showed thin linear lymphatic vessels and small dotted capillaries in the small villi (Fig. 4-A and -B). Jejunum revealed large dilated lymphatic vessels and small capillaries in the tall villi (Fig. 4-C and -D). Frozen sections of large intestine showed linear vertically spreading lymphatic vessels through the smooth muscle layers (Fig. 4-E). The presence of this vertically spreading lymphatic vessel provides spreading of colonic cancer cells through the vertical lymphatic vessels in the colonic smooth muscle layer, which is used for staging colonic cancer by Dukes histopathological classification including stage A (limited to the mucosa), B1 (involving smooth muscle layer but not penetrating it) and B2 (penetrating through smooth muscle layer)[26,27]. There were dispersed small blood vessels in lamina propria while there were many large arteries and veins in the submucosa (Fig. 4-E and -F). The formalin-fixed and paraffin-embedded normal colon immunostained some linear lymphatic vessels in the lamina propria and abundant lymphatic vessels in the submucosa (Fig. 4-G). Kennedy et al reported absent lymphatic vessels in lamina propria of normal colon with some lymphatic vessels in many cases with inflammation and neoplasia[27,28]. We believe the reported absence of lymphatic vessels in lamina propria was due to non-optical preservation of lymphatic vessels in paraffin-embedded large intestinal sections. Lymphangiogenesis was observed in benign colonic polyps and at the marginal zone of colonic carcinoma, some of which was immunostained for both LYVE-1 and vWF[30]. Furthermore, lymphangiogenesis occurs in adult tissue during inflammation, wound healing, tumorigenesis, and tumor invasion (3,4).

The hepatic sinusoids were positively immunostained for LYVE-1, but not in all zones on the paraffin-embedded sections were immunostained for LYVE-1 where oxygen-rich zone 1 (periportal hepatocytes) was negative in paraffin-embedded sections while oxygen-poor zones 2 and 3 (pericentral hepatocytes) were LYVE-1 positive (Fig. 3-B). In our study, all zones 1 to 3 were positively immunostained for LYVE-1 in the frozen sections

(Fig. 3-A). There are two types of sinusoidal epithelia in hepatocytes. Type1 sinusoidal epithelia are LYVE-1$^{-}$, CD34$^{hi}$CD14 hepatocytes in the oxygen-rich zone 1, and type 2 sinusoidal epithelia are LYVE-1$^{+}$, CD32$^{hi}$CD14$^{+}$CD36$^{mid\text{-}lo\ in}$ the oxygen-poor zone 2 and 3 hepatocytes (Fig. 3-A and -B) (31-34). So, LYVE-1 immunostaining was mostly stronger stained in the zones 2 and 3, which are venous capillaries with more LYVE-1 attached in the endothelia while zone 1 is arterial capillary with less LYVE-1 attached. Hepatic sinusoids are large capillaries being positive for LYVE-1 in zones 2 and 3 in paraffin-embedded sections but only patchy immunostained for vWF in the literature[31-34]. vWF immunostaining was negative in hepatic sinusoids in our study (Fig. 3-C). Since all undamaged endothelia of veins and arteries were positively stained for vWF in our study, vWF was not necessarily attached to the damaged vascular endothelium, but it was attached to the undamaged endothelia as well. In paraffin-embedded sections, zone 1 was positive and zone 2 was reportedly negative for CD34 since CD34 stained stronger for arteries than venules, supporting zone 1 as arterial capillary[33,34].

As described above, spleen, lymph node and liver all contain sinusoidal system. Hepatic sinusoids are like splenic sinuses in structure and function. Blood is screened through the sinus and is massively stored when the organs are congested under portal hypertension.

Pancreas showed different immunostaining patterns between frozen sections and paraffin-embedded sections: frozen sections showed very weak staining for LYVE-1 in islets while paraffin-embedded sections showed stronger staining islets[35]. In the paraffin-embedded sections, pancreatic neuroendocrine tumors (Pan-NETs) including non-functioning pancreatic NETs, metastatic insulinoma to liver and metastatic gastrinoma to lymph node were negative for LYVE-1 while pancreatic islets and lymphatic vessels in the normal pancreatic tissue, hepatic sinusoids and lymphatic sinusoids were all positively stained for LYVE-1[32,35]. In contrast, many pancreatic NETs were positively immunostained for lymphatic vessels using D2-40 (Figure not shown)[32-37]. So, this LYVE-1 positive immunostaining in islets supports that islets are lymphatic fluid-filled organ without lymphatic vessels, which function in the paracrine endocrine system since all four pancreatic hormones are interacting each other stimulating or inhibiting the secretion of the other hormones to maintain glucose homeostasis. In the paracrine islet system, insulin inhibits glucagon, glucagon stimulates insulin secretion, somatostatin inhibits insulin, glucagon, and pancreatic polypeptide secretion[37]. The absence of LYVE-1 immunostaining in pan-NETs supports a lack of paracrine system in Pan-NETs, which has no regulatory inhibitory secretory system in Pan-NETs [35,36]. Frozen sections of pancreas showed numerous baskets of vWF positive capillaries around and inside the islets, revealing numerous fenestrated capillaries in the islets positively immunostained with vWF in full thickness (Fig.4-F), which were not immunostained with paraffin-embedded sections (Figure not shown). Pancreatic islets occupy only 1 – 2% of the pancreas in volume but receive 5% to 20% of the total blood supply of the organ [38], which is supported by the presence of numerous capillaries around and in the islets.

The fine fibrous septum of the thyroid contained numerously scattered, small, linear lymphatic vessels and there were larger blood vessels in the broader fibrous septum (Fig. 5-A and -B). The thyroid contains numerous small lymphatic vessels and larger blood vessels as revealed by a classic dye injection study in the dog, in which numerous small lymphatic vessels were detected in the thin fibrous septa[39]. Ovarian sections showed diffusely distributed, numerous small lymphatic and blood vessels around the Graafian follicles in the stroma (Fig. 5-C and -D). The development and remodeling processes of ovarian blood and lymphatic vessels occur associated with cyclic remodeling[40]. The lymphatic drainage pathways of ovaries run via the ovarian and uterine ligaments and ovarian cancer may spread through lymphatic vessels to sentinel nodes, paraaortic and para-internal iliac arterial lymph nodes[41]. The prostate showed numerous small LYVE-1 positive

lymphatic vessels in the capsule and interstitial septa, where there were more numerous, diffusely scattered linear small blood vessels (Fig. 5-E and -F). The double immunohistochemical staining for lymphatic and blood vessels revealed numerous CD34 positive blood vessels but only a few LYVE-1 positive lymphatic vessels in the benign prostatic hyperplasia and prostatic carcinoma, in which the destruction of lymphatic vessels and angiogenesis occur simultaneously[42,43]. The rich lymphatic vessels in the capsule may facilitate lymphatic spread of prostatic cancer[44]. There were abundant nerve bundles in the capsule (Fig. 5-E and –F).

Frozen sections of adrenal gland showed many small lymphatic vessels and larger blood vessels in the subcapsular tissue, and neither LYVE-1 and vWF immunostaining revealed lymphatic and blood vessels in the cortex (Fig. 6-A and -B). Adrenal gland receives blood from 30 to 50 small arteries which penetrate the capsule at different points and form capillary plexus of arterioles. These arterioles supply the capillaries that extend vertically to the cortex and separate the cords of cortical cells[45]. Frozen sections of the kidney showed a strikingly different distribution of lymphatic and blood vessels between cortex and medulla: there were a few lymphatic vessels at the arterial adventitia in the cortex while there were numerous small lymphatic vessels adjacent to the ample blood vessels in the medulla (Fig. 4-C and -E). Glomerular capillaries, which were fenestrated capillaries, were diffusely immunostained in full thickness, supporting that glomerular capillaries were leaking serum through blood vessels immunostained by this vWF staining and larger blood vessels were stronger immunostained than smaller vessel endothelia (Fig. 4-D). Glomerular endothelia were positive for CD31 and CD34 but negative for vWF in the paraffin-embedded sections (4,46,47) but were positive for vWF and negative for LYVE-1 in the frozen sections[4]. Thus, glomerular endothelia were positively stained in the frozen sections for vWF but not in the paraffin-embedded sections[4]. The Bowman's capsule was immunostained for D2-40 (Fig. 7-F). Pusztaszeri et al reported completely negative staining in glomerular endothelium for F-8 but were positively stained by CD31 and CD34 in the paraffin-embedded sections[4]. This is the major difference in immunostaining of glomerular endothelium between frozen sections and paraffin-embedded sections. In the urinary bladder, there were dispersed small lymphatic and blood vessels in the muscularis mucosa while smooth muscle layers revealed some dispersed lymphatic and blood vessels (Fig. 7-G and -H). Thus, ample small blood and lymphatic vessel networks are present in the urinary bladder[48], which may contribute to lymphatic and hematogenous spread of bladder cancer to the distant organs[49].

## Conclusion

Frozen sections of spleen revealed large LYVE-1-positive sinusoidal capillaries and small vWF-positive sinusoidal capillaries, the latter were not detected in the paraffin-embedded sections. Normal colonic lamina propria was reportedly missing for lymphatic vessels with paraffin-embedded sections[26,27]. However, the frozen section revealed lymphatic vessels in the normal colonic lamina propria (Fig. 3-E). Hepatic sinusoids are conventionally divided into oxygen-poor LYVE-1-positive zones 2 and 3 and oxygen-rich, LYVE-1-negative periportal zone 1[29-32]. With frozen sections, all three zones 1 -3 were LYVE-1 positive with zones 2 and 3 being stronger immunostained than zone 1 (Fig. 4-A and -B).

More striking findings were revealed for blood vessels with frozen section immunostaining using vWF as a blood vessel marker. Immunostaining for vWF was positive for damaged blood vessels but negative for non-damaged normal blood vessels with conventional immunostaining using formalin-fixed and paraffin-embedded sections[4]. Immunostaining with frozen sections revealed positive staining for vWF in both normal, non-damaged veins and arteries (Fig. 2-D and-F, Fig. 3-F). Immunostaining with the frozen sections revealed positive staining in the alveolar sac and margin of muscle bundles of the diaphragm (Fig. 2-E and -F). The striking vWF positive immunostaining was

observed in the baskets of numerous small capillaries in the pancreatic islets (Fig. 4-F) and diffusely vWF positive immunostaining in the glomerular capillaries in full thickness, and these two findings were only obtained with frozen sections and had not been reported with the formalin-fixed and paraffin-embedded immunostaining.

Thus, immunohistochemical staining with frozen sections is superior to conventional immunohistochemical staining with formalin-fixed and paraffin-embedded sections and has provided new information on lymphatic and blood vascular system in the normal organs, which has not been reported before and more new information will be forthcoming by immunohistochemical staining using frozen sections.

## Conflict of Interest Statement:

None

## Acknowledgements:

We want to express our sincere thanks to Drs. OV Slayden and Robert Brenner for allowing us to use their research laboratory for this project at the Oregon National Primate Research Center, Beaverton, OR, USA.

## References:


1. Kong, LL, Yang, NZ, Zhao, GH, Zhou, W et al" The optimum marker for the detection of lymphatic vessels (Review). Moll Cell Oncology 2017, 7(4):515 -520.

2. Muller, AM, Hemanns, MI, Skrzynski, C, Messlinger, M, Muller, KM et al: Expression of the endothelial markers PECAM-1, vWf and CD34 in vivo and in vitro. Exp Mol Pathol 2001, 72(34):221-229.

3. Scarvelli, C, Weber, E, Agliano, M, Cirulli, T, Nico, B et al: Lymphatics at the crossroads of angiogenesis and lymphangiogenesis. J Anat 2004, (6):433-449.

4. Pusztaszeri, MP, Seelentag, W, Bosman, FT, Immunohistochemical expression of endothelial markers CD31, CD34, bon Willebrand factor, and Fli in normal human tissues. J Histochem Cytochem 2006, 54(4):385-395.

5. Jackson, DG, Prevo, R, Clasper, S, Bonerji, S: LYVE-1, the lymphatic system and tumor lymphangiogenesis. Trend Immunol 2001, 22(6): 317-321.

6. Jackson, DG: The lymphatics revisited. New perspectives from the hyaluronan receptor LYVE-1. Trend Cardiovasc Med 2003, 13(1):1-7.

7. Tammala, T, Alitalo, K: Molecular mechanisms and future promise. Cell 2010, 140(4):460-476.

8. Zheng, W, Asspelund, A, Alitalo, K: Lymphangiogenetic factors, mechanisms, and application. Lab Invest 2014, 124(3):878-887.

9. Tomita, T: Immunocytochemical localization of lymphatic and venous vessels in colonic polyps and adenomas. Dig Dis Sci, 53(11):1880-1885.

10. Tomita, T: Cancer-associated lymphatic and venous vessels in colonic carcinomas. Open J Pathol 2014, 4(2);101-109.

11. Tomita, T: Immunohistochemical staining for lymphatic and blood vessels in normal tissues with frozen sections. Structure and Function Relationship. J Histolol Histopathol 2023, 10(1):1-8.

12. Slayden, OD, Koji, T, Brenner, RM: Microwave stabilization enhances immunocytochemical detection of estrogen receptor in frozen endothelial cells and lymphatic vessels to grow and invade. Cancer Res 1995, 136(6):4012-4021.

13. Slayden, OD, Brenner, RM: A critical period of progesterone withdrawal precedes menstruation in macaques. Reprod Biol Endocrinol 2006, 4 (Suppl 1): s6.

14. Cao, W, Mah, K, Caroll, RS, Slayden OD, Brenner, RM: Progesterone withdrawal up-regulates fibronectin and integrins during menstruation and repair in the rhesus macaque endometrium. Hum Reprod 2007, 22(12):3223-3231.

15. Giorno, R: Unusual structure of human splenic sinusoids revealed by monoclonal antibodies. Histochem 1984, 81(9):505-507.

16. Johnson, V,:Comparison an definition of spleen and lymph node: A phylogenetic analysis. J Theor Biol, 1985, 117(4):691-699.

17. Borch, WR, Aguileera, NS, Brussette, MD, O'Malley, A: practical application in immunohistochemistry. An immunophonetypic approach to the spleen. Arch Path Lab Med 2019, 143(9):1093-1105.

18. Rajajska, A, Gula, G, Flaht-Zabost, A, Czarnowska, E, Ciszek, B et al: Comparative and developmental anatomy of cardiac lymphatics. Scientific World Journal 2014, Article ID 183170.

19. Shimada, T, Zhang, L, Abe, K, Yamabe, M, Miyamoto, T: Developmental morphology of blood and lymphatic capillary networks in mammalian hearts, with special reference to three-dimensional architecture. Ital J Anat Embryol 2001, 106(s Suppl 1):203-211.

20. Weber, E, Sozio, F, Borghni, A, Sestini, P, Renzoni, E: Pulmonary lymphatic morphology: a review. Ann Anat 2018, 218(4):110-117.

21. Aiyama, S, Kikuchi, K, Tanaka, K, Ikeda, R, Sato, S et al: Immunohistochemical study of the lymphatic vessels in major salivary glands of the rat. Okajima Folia Anat Jpn, 2011, 87(4):177-180.


 

22. Yajin, S, Murakami, G, Takeuchi, H, Hasegawa, T, Kitano, H: The normal configuration and interindividual differences in intramural lymphatic vessels of the esophagus. J Thorac Cardiovasc Surg 2009, 137(6):1406-1414.

23. Merkin, RJ: Suprarenal gland lymphatic drainage. Am J Ana 1966, 119:359-374.

24. Howell, GM, Gray, SE, Armstrong, MJ, Stang, MT, McCoy, K et al: Outcome and prognostic factors after adrenalectomy for patients with distant adrenal metastasis. Ann Sur Oncol 2013, 20(11): 3491-3496.

25. Bazhennnova, L, Newton, P, Mason, J, Bethel, K, Nieva, j et al: Adrenal metastasis in lung cancer: Clinical implications of a mathematical model. J Thor Oncol 2014, 9(4):442-446. 8079-8084.

26. Jass, JR, Morson, BC: Reporting colorectal carcinoma. J Clin Patol 1987, 40(9):1016-1023.

27. Shepherd, NA, Saraga, EP, Love, JB, Jass, JR: Prognostic factors in colonic cancer. Histopathology, 1989, 14(6):613-620.

28. Kenndy, BC, Jain, D: Identification of lymphatics within the colonic lamina propria in inflammation and neoplasia using monoclonal antibody D2-40. Yale J Biol Med 2008,81(3):101-113.

29. Alexander, JS, Ganda, UC, Jordan, PA, Witte, MH: Gastrointestinal lymphatics in health and disease. Pathophysiol 2010,17(10):315-335.

30. Tomita, T: Immunocytochemical localization of lymphatic and venous vessels in colonic polyps and adenomas. Dig Dis Sci, 2008,53 (7):1880-1885.

31. Mouta-Carreita, C, Nasser, SM, de Tomaso, E, Padera, TP, Boucher, Y: LYVE-1 is not restricted to the lymph vessels: Expression in normal liver blood sinusoids and down-regulated in human liver cancer and cirrhosis. Cancer Res 2001, 61(22): 8079-80884.

32. Straus, O, Phillips, A, Roggiero, K, Barlett, A: An immunofluorescence identifies distinct subsets of endothelial cells in human liver. Sci Rep 2017, March 17, 44356.

33. Do, H, Healey, JF, Waller, EK, Lollar, P: Expression of factor VIII by murine liver sinusoidal epithelial cell. J Biol Chem 1999, 274(28):19587-19592.

34. Knolle, PA, Wohlleber, D: Immunological function of liver sinusoidal endothelial cells. Cell Mol Immunol 2016, 13(4):347-353.

35. Tomita, T: Lymphatic vessel endothelial hyaluronan 1 immunohistochemical staining for pancreatic islets and pancreatic endocrine tumors. Pancreas 2007, 35(4): e18-e22.

36. Tomita, T: D2-40 immunocytochemical staining for pancreatic islets and pancreatic endocrine tumors. Modern Pathol 2009, 38(11);339-341.

37. Tomita, T: New markers for pancreatic islets and islet cell tumors. Pathol Int 2002, 52(7):425-432.

38. Jansson, L, Barbu, A, Drotte, CJ, Espes, D, Gao, X: Pancreatic islet blood supply and its measurement. Upsala J Med Sci 2016, 12(2):81-95.

39. Johnson, M: The lymphatic system and thyroid connection. Thyroid Nation, July 31, 2018. 40. Brown, HM, Robker, RL, Russell, DL: Development and hormonal regulation of the ovarian lymphatic vasculature. Endocrinol 2010, 2010, 151(11):5446-5455.

41. Kleppe, M, Kraima, AC, Kruitwagen, R, Van Gorp, T, Smit, NN et al: Understanding lymphatic drainage pathways of the ovaries to predict site for sentinel nodes in ovarian cancer. Int J Gynecol Cancer 2015, 25(8):140501414.

42. Trojan, L, Michel, MS, Rensch, F, Jackson, DG, Alken, P et al: lymph and blood vessel architecture in benign and malignant prostatic tissue: Lack of lymphangiogenesis in prostate carcinoma assessed with novel lymphatic marker lymphatic vessel endothelial hyaluronan receptor LYVE-1. J Urol 2004,172(1):103-107.

43. Zeng, Y, Opeskin, K, Horvath, LG, Sutherland, RL, Williams, EP: Lymphatic vessel density and lymph node metastasis in prostatic cancer. Prostate 2005, 10(15):5137-5144.

 

44. Lucini, C, Fleishman, A, Beermans, J, Fassan, M, Nottegar, A et al: Extranodal extension of lymph node metastasis influence recurrence in prostatic cancer: Systematic review and meta-analysis. Sci Rep 2017, 7(1):2374.

45. Netter, F: Adrenal gland. In: Endocrine system and selected metabolic diseases. Vol.4, pp 77-108, CIBA collections of medical illustration, CIBA Pharmaceutical Company, NY 1965.

46. Russel, PS, Hong, J, Windsor, JA, Itkin, M, Phillips, J: Renal lymphatics: Anatomy, physiology, and clinical implications. Front Physiology and Pathophysiology, 14 March, 2019.

47. Ishikawa, Y, Akasaka, Y, Kiguchi, H, Akishima-Fukasawa, Y, Hasegawa, t et al: Human renal lymphatics under normal and pathological conditions, Histopathol 2006, 49(8):265-273.

48. Standing, S: Urinary bladder: the anatomical basis of clinical practice. In: Gray's anatomy, pp 1255-1261, 2016, Philadelphia.

49. Ku, JH, Kang, M, Kim, HS, Jeong, CW, Kwok, C et al: Lymph node density a prognostic variable in node-positive bladder cancer: a meta-analysis. BMC Cancer 2015, Jan. 2:15:447.